Figure S1

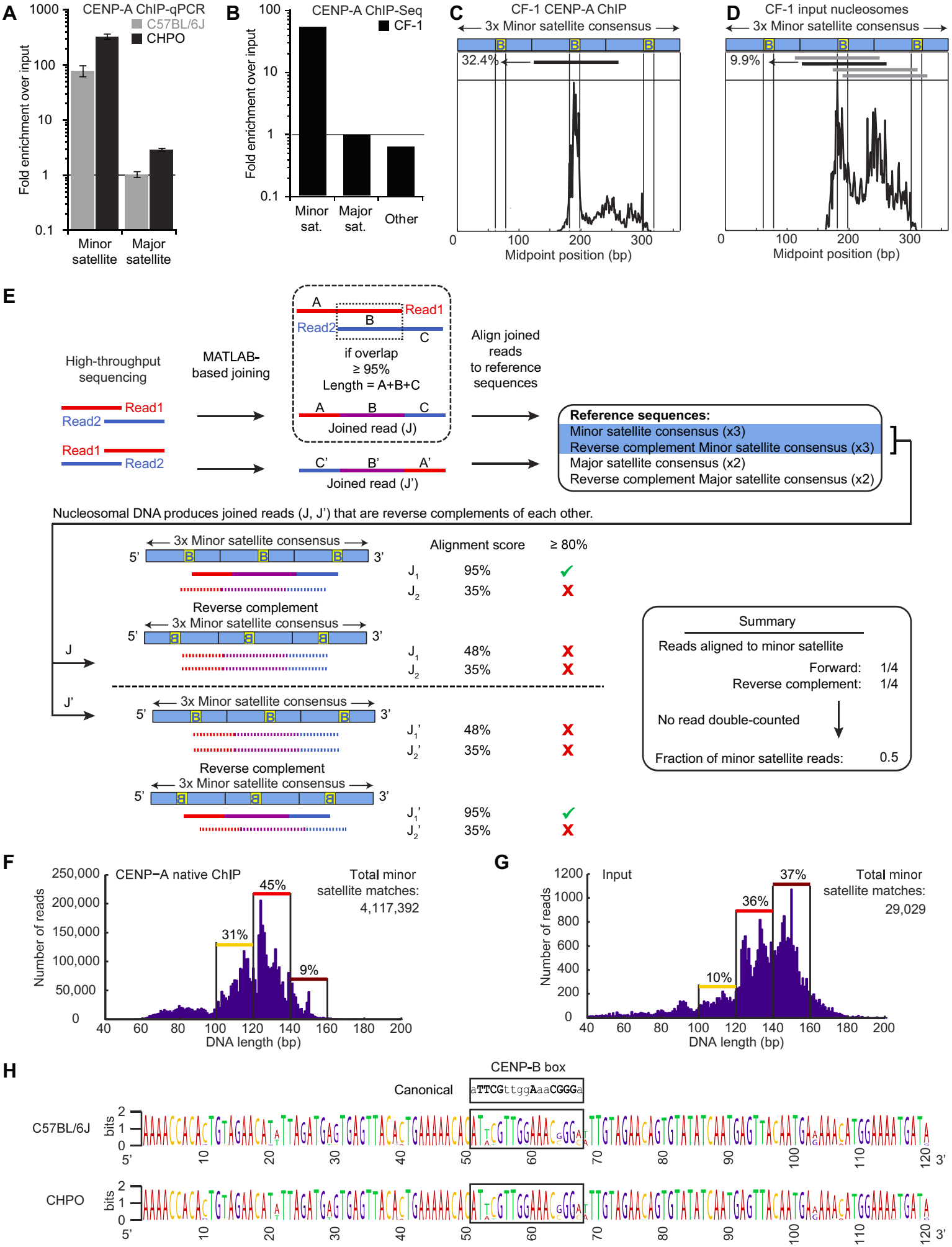
A
CENP-A ChIP-qPCR
C57BL/6J
CHPO
Fold enrichment over input
Minor satellite
Major satellite
B
CENP-A ChIP-Seq
CF-1
Minor sat.
Major sat.
Other
C
CF-1 CENP-A ChIP
3x Minor satellite consensus
32.4%
Midpoint position (bp)
D
CF-1 input nucleosomes
9.9%
E
High-throughput sequencing
MATLAB-based joining
Read1
Read2
if overlap ≥ 95%
Length = A+B+C
Joined read (J)
Joined read (J')
Align joined reads to reference sequences
Reference sequences:
Minor satellite consensus (x3)
Reverse complement Minor satellite consensus (x3)
Major satellite consensus (x2)
Reverse complement Major satellite consensus (x2)
Nucleosomal DNA produces joined reads (J, J') that are reverse complements of each other.
Alignment score
≥ 80%
Reverse complement
Summary
Reads aligned to minor satellite
Forward: 1/4
Reverse complement: 1/4
No read double-counted
Fraction of minor satellite reads: 0.5
F
CENP-A native ChIP
Total minor satellite matches: 4,117,392
Number of reads
DNA length (bp)
G
Input
Total minor satellite matches: 29,029
H
CENP-B box
Canonical
C57BL/6J
CHPO
bits

Figure S2

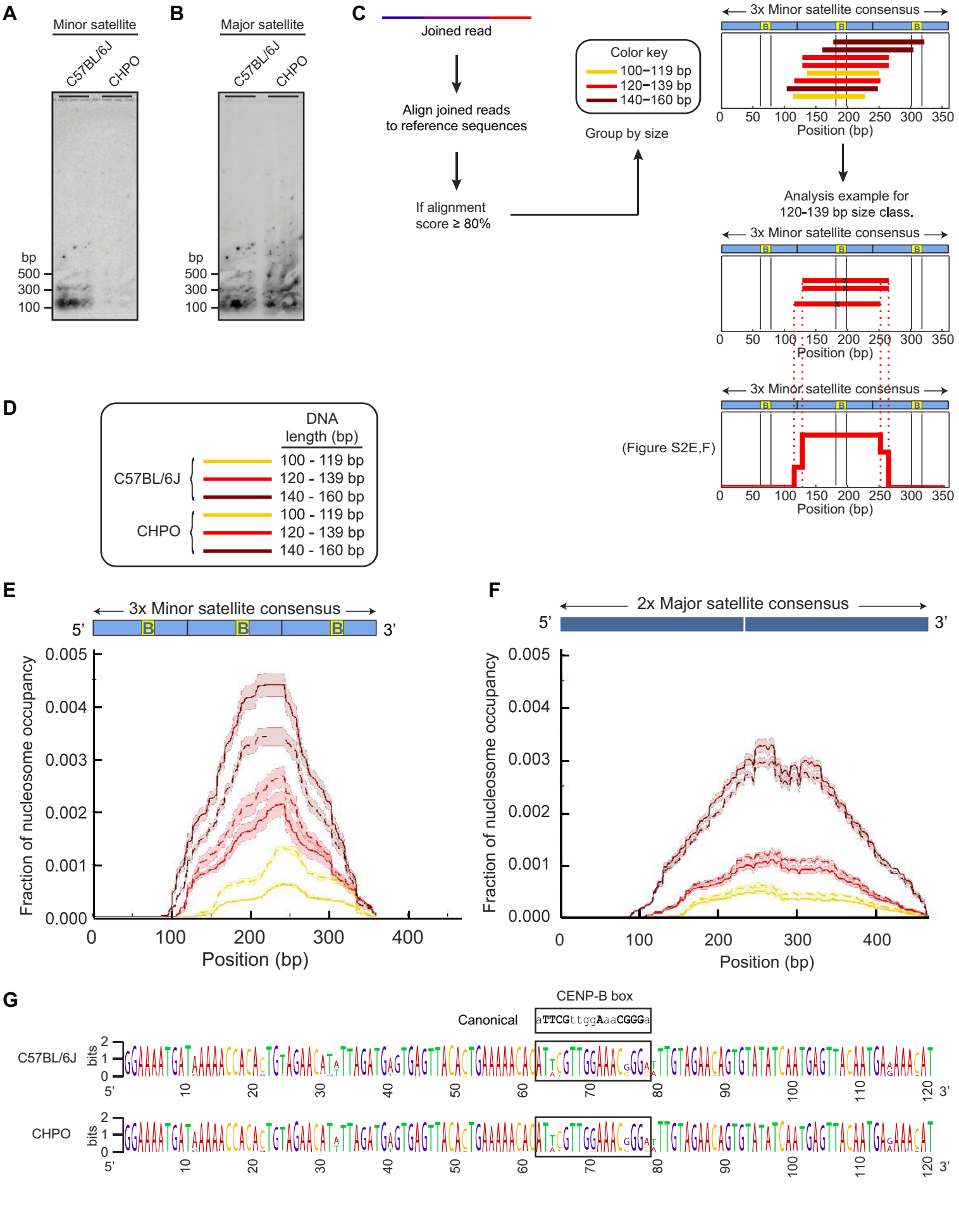
A
Minor satellite
C57BL/6J
CHPO
bp
500
300
100
B
Major satellite
C57BL/6J
CHPO
bp
500
300
100
C
Joined read
Align joined reads to reference sequences
If alignment score ≥ 80%
Color key
100–119 bp
120–139 bp
140–160 bp
Group by size
3x Minor satellite consensus
B
0 50 100 150 200 250 300 350
Position (bp)
Analysis example for 120-139 bp size class.
(Figure S2E,F)
D
DNA length (bp)
C57BL/6J
100 - 119 bp
120 - 139 bp
140 - 160 bp
CHPO
100 - 119 bp
120 - 139 bp
140 - 160 bp
E
3x Minor satellite consensus
5'
3'
Fraction of nucleosome occupancy
0.005
0.004
0.003
0.002
0.001
0.000
0 100 200 300 400
Position (bp)
F
2x Major satellite consensus
5'
3'
Fraction of nucleosome occupancy
0.005
0.004
0.003
0.002
0.001
0.000
0 100 200 300 400
Position (bp)
G
CENP-B box
Canonical
aTTCGttggAaaCGGGa
C57BL/6J
CHPO
bits
2
1
0
5'
10 20 30 40 50 60 70 80 90 100 110 120
3'

Figure S3

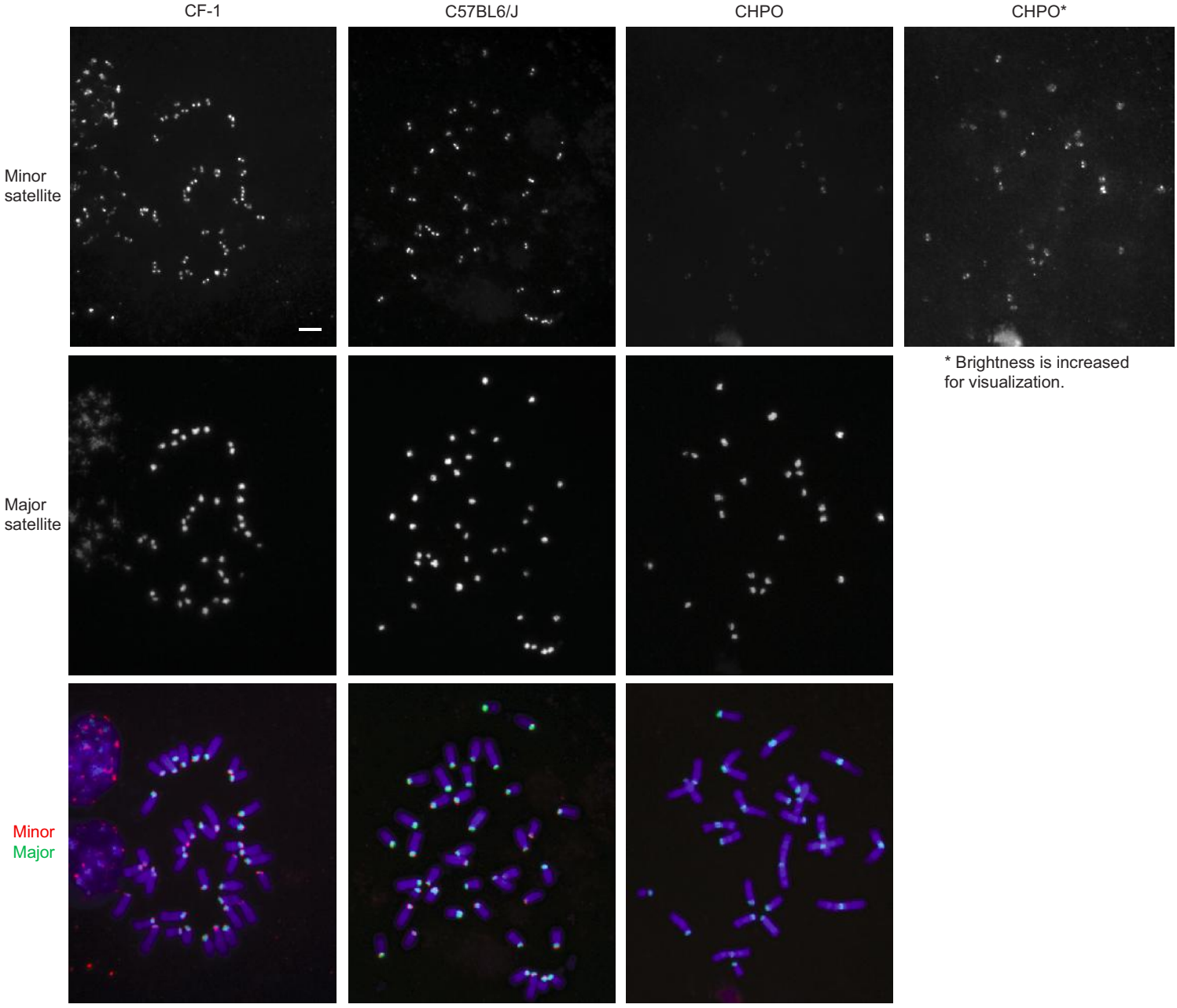
CF-1
C57BL6/J
CHPO
CHPO*
Minor satellite
Major satellite
Minor
Major
* Brightness is increased for visualization.

Figure S4

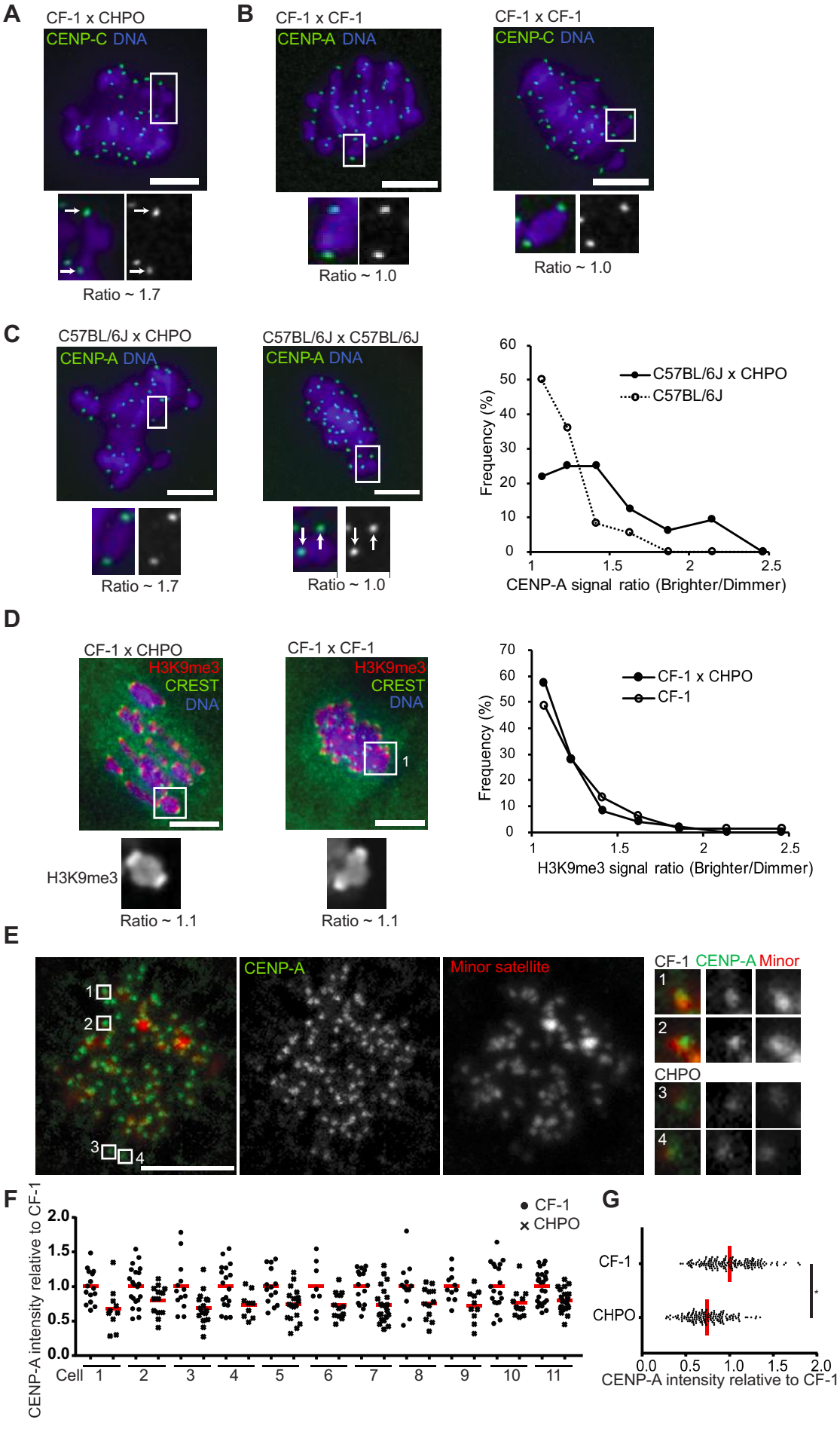
A
CF-1 x CHPO
CENP-C DNA
Ratio ~ 1.7
B
CF-1 x CF-1
CENP-A DNA
Ratio ~ 1.0
CF-1 x CF-1
CENP-C DNA
Ratio ~ 1.0
C
C57BL/6J x CHPO
CENP-A DNA
Ratio ~ 1.7
C57BL/6J x C57BL/6J
CENP-A DNA
Ratio ~ 1.0
C57BL/6J x CHPO
C57BL/6J
Frequency (%)
CENP-A signal ratio (Brighter/Dimmer)
D
CF-1 x CHPO
H3K9me3
CREST
DNA
H3K9me3
Ratio ~ 1.1
CF-1 x CF-1
H3K9me3
CREST
DNA
Ratio ~ 1.1
CF-1 x CHPO
CF-1
Frequency (%)
H3K9me3 signal ratio (Brighter/Dimmer)
E
CENP-A
Minor satellite
CF-1 CENP-A Minor
CHPO
F
CF-1
CHPO
CENP-A intensity relative to CF-1
Cell
G
CF-1
CHPO
CENP-A intensity relative to CF-1

**Supplemental Figure Legends:**

**Figure S1. Mouse CENP-A nucleosomes are highly phased and protect a shorter length of DNA from MNase digestion relative to the total (input) nucleosome population. Related to Figure 1.**

(A) Minor satellite DNA is enriched for weaker centromeres to a greater extent than for stronger centromeres following CENP-A native ChIP. Quantitative real-time PCR analysis of stronger (C57BL/6J) and weaker (CHPO) CENP-A ChIP DNA. CENP-A ChIP signals for minor and major satellite are represented as the fold increase in signal relative to input signal (mean±SEM, n=3 independent experiments).
(B) CENP-A ChIP sequencing results for CF-1. Fold-enrichment was calculated as the fraction of reads that are minor or major satellite in the ChIP sample divided by the fraction in the input sample (n=1).
(C-D) Midpoint position of CF-1 CENP-A ChIP (B) or input (C) reads (size 100-160 bp) along the trimer minor satellite consensus sequence. Vertical lines indicate the 17-bp CENP-B box. The major CENP-A nucleosome position (identified across CENP-A ChIP samples) is indicated by a horizontal black line above the respective midpoint value. The same nucleosome position is indicated in the input sample. Numbers to the left of the positions indicate the percentage of reads (n=1) where the midpoint spans the 10 bp at the 3' end of the CENP-B box (yellow, labeled B). Horizontal gray lines indicate other major nucleosome positions in the input samples.
(E) Schematic for tandem repeat analysis of paired-end sequencing reads. (Top) High-throughput sequencing of Illumina libraries prepared from nuclease-protected chromatin produces paired-end reads (Read1, Read2). Paired-end reads are joined in MATLAB using the 'localalign' function to determine the overlapping region between the paired-end reads (requiring ≥95% overlap identity, see [S1], and adapter sequences are removed if present. Each double-stranded nucleosomal DNA produces joined reads (J and J') that are reverse complements of each other. (Bottom) Joined reads are aligned against a series of reference sequences (either a trimer of minor satellite consensus sequence or a dimer of major satellite consensus sequence or to the reverse complement of those tandem consensus sequences). Alignment against the minor satellite consensus and the corresponding reverse complement are diagrammed. Those joined reads aligning with ≥ 80% identity are chosen for further analysis. Two illustrative examples of sets of joined reads are depicted. $J_1$ and $J_1$' originated from the same double-stranded nucleosomal DNA and align to the forward and reverse complement minor satellite consensus sequences, respectively. The second set, $J_2$ and $J_2$', do not align. (Summary) The fraction of total reads reported (e.g. Figure 2D) is the number of joined reads aligning to the consensus sequence in either the forward or reverse complement orientation (without double-counting any joined read) divided by the total number of joined reads.
(F-G) CENP-A nucleosomes protect shorter lengths of DNA from MNase digestion relative to input nucleosomes. Length distribution of nuclease-protected DNA fragments from C57BL/6J CENP-A native ChIP (F) or input (G) that align to the minor satellite consensus sequence with ≥80% identity. Note that there is a higher prevalence of short reads (100-119 bp) and lower prevalence of long reads (140-160 bp) for CENP-A ChIP relative to input, consistent with observations in human [S1].

(H) The minor satellite monomer sequence of well-positioned CENP-A ChIP reads is similar between weaker and stronger centromeres. To detect potential differences in the sequences of minor satellite monomers between stronger (C57BL/6J) and weaker (CHPO) centromeres, we performed multiple sequence alignment of minor satellite reads from CENP-A ChIP-seq with midpoint values at the CENP-B box from stronger (C57BL/6J) and weaker (CHPO) strains. At each position along the 120-bp monomer, sequence conservation is represented as the overall height, with individual heights indicating the relative frequency of each nucleic acid. The position of the 17-bp CENP-B box is highlighted. The sequence of the canonical CENP-B box motif is indicated above the sequence logos, and residues required for CENP-B binding appear as capital letters [S2].

**Figure S2. Stronger centromeres (C57BL/6J) contain more minor satellite than weaker centromeres (CHPO), which are characterized by a high proportion of shorter minor satellite nucleosome lengths. Related to Figure 2.**

(A-B) Southern blot of MNase-digested chromatin. To ensure that our MNase-seq accurately represents genomic satellite DNA in stronger (C57BL/6J) and weaker (CHPO) strains, we performed a Southern blot of the MNase-digested chromatin that served as the input for our Illumina library preparation. Equal amounts of MNase-digested DNA from stronger (C57BL/6J) and weaker (CHPO) strains were probed consecutively for minor (A) and major satellite (B) DNA (n=3 independent samples). Both minor (A) and major satellite (B) DNA are found predominantly as a mononucleosome species, from which the whole genome sequencing libraries were prepared, for both strains, ruling out a potential bias. Note that while major satellite signals (B) are similar for the two strains, the minor satellite signals (A) are much lower for the weaker centromere strain, consistent with our complementary FISH analysis (Figure 2E-G) and the conclusion that weaker centromeres have less minor satellite DNA than stronger centromeres.
(C-F) Shorter minor satellite nucleosome lengths make up a higher proportion of weaker centromeres relative to stronger centromeres. (C) Schematic depicting nucleosome occupancy analysis. Joined reads that align to the reference sequence with ≥80% identity were sorted according to midpoint value and grouped by size. The position of each nucleosome along the multimerized consensus sequence (here minor satellite) was plotted as a horizontal line and color-coded by length, as indicated (top). As an analysis example, the positions of the 120-139 bp reads are replotted with midpoints indicated with an 'x' (middle). The number of reads that overlap at each particular base pair along the position coordinate are summed and plotted to yield the nucleosome occupancy map (below). Dashed red lines connect the edges of the fragment positions (middle) with the corresponding heights in the nucleosome occupancy map (below). (D) Color key for nucleosome occupancy maps. (E-F) Nucleosome occupancy maps for the three different size classes of nucleosomes from MNase-seq along the length of the minor (E) or major (F) satellite consensus from stronger (C57BL/6J, solid lines) and weaker (CHPO, dashed lines) centromeres (mean±SEM, n=3 independent experiments). Note the higher proportion of short nucleosomal DNA lengths (100-119 bp) for minor satellite in CHPO relative to C57BL/6J, while major satellite nucleosome lengths are similar between the strains.
(G) The minor satellite monomer sequence is similar between weaker and stronger centromeres. Multiple sequence alignment of minor satellite MNase-seq reads from

stronger (C57BL/6J) and weaker (CHPO) strains. At each position along the 120-bp monomer, sequence conservation is represented as the overall height with individual heights indicating the relative frequency of each nucleic acid. The position of the 17-bp CENP-B box is highlighted. The sequence of the canonical CENP-B box motif is indicated above the sequence logos, and residues required for CENP-B binding appear as capital letters [S2]. Note that the minor satellite multiple sequence alignments for Figures S1H and panel G of this figure are not in the same register. The preferred positions of the CENP-A nucleosomes on the minor satellite DNA (Figures 1C,E) in the former (Figure S1H) is not present in the latter (Figure S2G) where the MNase-seq sequences used for the sequence logo analysis mostly derive from canonical nucleosomes that don't have such preferred midpoint positions.

**Figure S3. Stronger centromeres (CF-1 and C57BL/6J) contain more minor satellite than weaker centromeres (CHPO). Related to Figure 2.**

Representative FISH images of minor satellite (red) and major satellite (green) on metaphase chromosomes (blue) of CF-1, C57BL/6J and CHPO. The same FISH images from C57BL/6J and CHPO in Figure 2E are shown here in grayscale for minor and major satellite signals. Scale bar, 5 μm.

**Figure S4. CENP-A and CENP-C levels are asymmetric across the bivalents in hybrid oocytes, and greater minor satellite abundance is associated with increased CENP-A levels. Related to Figure 4.**

(A-B) Representative images of CENP-C staining in a CF-1 x CHPO oocyte (A), and CENP-A and CENP-C staining in CF-1 oocytes (B), corresponding to the quantification in Figure 4B.
(C) Representative images of CENP-A staining in C57BL/6J x CHPO and C57BL/6J oocytes.
(D) Representative images of H3K9me3 and CREST staining in CF-1 x CHPO and CF-1 oocytes. Graphs are histograms of CENP-A (C) or H3K9me3 (D) intensity ratios, calculated as the brighter divided by the dimmer signal for each bivalent. Images are maximal intensity z-projections; insets are optical slices showing single bivalents (arrows indicate paired centromeres). Scale bars, 10 μm.
(E) Representative images of CENP-A staining and minor satellite FISH in CF1 x CHPO hybrid embryonic fibroblast cells. Cells were treated with a kinesin-5 inhibitor (STLC) to generate monopolar spindles to disperse the chromosomes. CF-1 (insets 1 and 2) and CHPO (insets 3 and 4) centromeres were distinguished based on intensity of minor satellite signals, which are weak or undetectable at CHPO centromeres. Note that two CF-1 centromeres have particularly high levels of minor satellite. Scale bar, 5 μm.
(F) CENP-A signals were quantified in eleven cells. Each dot represents one centromere; red bar, mean.
(G) Data from all eleven cells are pooled; red bar, mean; * $p < 0.0001$.

**Table S1. Analysis of reads from CENP-A ChIP-seq shows no enrichment of annotated repetitive elements that could have formed an alternative centromere assembly site. Related to Figure 1.**

| | C57BL6/J[a] | | | | | | | | | CHPO[a] | | | | | | | | |
|---|---|---|---|---|---|---|---|---|---|---|---|---|---|---|---|---|---|---|
| Repeat name[b] | Number of elements[c] | | | | | | Fold-enrichment[d] | | | p[e] | Number of elements[c] | | | | | | Fold-enrichment[d] | | | p[e] |
| | CENP-A ChIP | | | INPUT | | | | | | | CENP-A ChIP | | | INPUT | | | | | | |
| Satellite-SATMIN[f] | 6038.7 | ± | 467.4 | 52.3 | ± | 2.9 | 115.7 | ± | 8.5 | 0.003 | 3120.0 | ± | 127.9 | 8.0 | ± | 2.1 | 444.0 | ± | 103.9 | 0.001 |
| Satellite-GSAT_MM[g] | 739.7 | ± | 71.1 | 799.3 | ± | 4.1 | 0.9 | ± | 0.1 | 0.749 | 2171.3 | ± | 86.0 | 784.0 | ± | 17.6 | 2.8 | ± | 0.0 | 0.001 |
| SINE/MIR-MIRb | 6.0 | ± | 2.9 | 9.0 | ± | 2.0 | 0.8 | ± | 0.4 | 0.705 | 7.3 | ± | 2.7 | 5.7 | ± | 2.7 | 2.6 | ± | 1.4 | 0.393 |
| Satellite/centr-CENSAT_MC | 2.0 | ± | 1.2 | 1.3 | ± | 0.3 | 2.0 | ± | 1.2 | 0.346 | 2.0 | ± | 0.0 | 0.0 | ± | 0.0 | ND | ± | ND | ND |
| Simple_repeat-(TA)n | 3.0 | ± | 1.5 | 4.0 | ± | 1.5 | 1.9 | ± | 1.6 | 0.629 | 2.3 | ± | 1.2 | 5.7 | ± | 0.3 | 0.4 | ± | 0.2 | 0.926 |
| SINE/Alu-PB1 | 1.3 | ± | 0.3 | 2.7 | ± | 1.3 | ND | ± | ND | ND | 4.3 | ± | 2.3 | 3.0 | ± | 2.0 | 1.8 | ± | 0.2 | 0.029 |
| Satellite-MMSAT4 | 0.7 | ± | 0.3 | 1.0 | ± | 0.6 | ND | ± | ND | ND | 1.7 | ± | 0.9 | 2.0 | ± | 1.0 | 1.7 | ± | 0.9 | 0.563 |
| Simple_repeat-(GA)n | 0.0 | ± | 0.0 | 1.3 | ± | 0.3 | 0.0 | ± | 0.0 | 0.971 | 2.3 | ± | 0.3 | 1.7 | ± | 0.3 | 1.7 | ± | 0.7 | 0.211 |
| LTR/ERVK-RMER13B | 2.0 | ± | 0.0 | 1.3 | ± | 0.3 | 1.7 | ± | 0.3 | 0.092 | 2.0 | ± | 0.6 | 2.0 | ± | 1.5 | ND | ± | ND | ND |
| LTR/ERV1-RLTR6-int | 2.7 | ± | 0.9 | 5.3 | ± | 2.6 | 1.6 | ± | 1.2 | 0.738 | 2.7 | ± | 0.3 | 6.3 | ± | 1.3 | 0.5 | ± | 0.1 | 0.921 |
| Simple_repeat-(TTG)n | 1.3 | ± | 0.7 | 4.0 | ± | 0.6 | 0.4 | ± | 0.2 | 0.922 | 3.7 | ± | 0.3 | 3.7 | ± | 1.5 | 1.6 | ± | 0.7 | 0.500 |
| LTR/ERVK-MMERVK9E_I-int | 2.7 | ± | 0.9 | 5.0 | ± | 2.3 | 1.5 | ± | 1.2 | 0.759 | 4.3 | ± | 0.9 | 8.3 | ± | 0.9 | 0.5 | ± | 0.2 | 0.940 |
| LTR/ERVL-MaLR-MLT1B | 0.7 | ± | 0.3 | 5.3 | ± | 0.9 | 0.1 | ± | 0.1 | 0.990 | 1.7 | ± | 1.2 | 1.7 | ± | 0.3 | 1.5 | ± | 1.3 | 0.437 |
| LINE/L1-L1MC1 | 0.0 | ± | 0.0 | 4.3 | ± | 2.0 | 0.0 | ± | 0.0 | 0.917 | 1.7 | ± | 1.2 | 1.7 | ± | 0.7 | 1.4 | ± | 1.3 | 0.500 |
| Simple_repeat-(TCTT)n | 0.3 | ± | 0.3 | 1.7 | ± | 0.3 | 0.2 | ± | 0.2 | 0.971 | 2.0 | ± | 0.6 | 2.0 | ± | 0.6 | 1.4 | ± | 0.8 | 0.500 |
| SINE/B2-B2_Mm1t | 3.3 | ± | 1.5 | 10.3 | ± | 2.0 | 0.3 | ± | 0.1 | 0.978 | 11.3 | ± | 2.9 | 8.7 | ± | 1.5 | 1.4 | ± | 0.5 | 0.280 |
| Low_complexity-G-rich | 3.7 | ± | 1.5 | 3.3 | ± | 0.9 | 1.4 | ± | 0.6 | 0.446 | 0.3 | ± | 0.3 | 1.7 | ± | 0.7 | 0.3 | ± | 0.3 | 0.865 |
| SINE/ID-ID | 1.7 | ± | 0.3 | 5.3 | ± | 0.9 | 0.3 | ± | 0.1 | 0.973 | 3.0 | ± | 1.0 | 2.3 | ± | 0.3 | 1.4 | ± | 0.6 | 0.317 |
| Simple_repeat-(G)n | 8.0 | ± | 2.3 | 13.0 | ± | 3.8 | 0.7 | ± | 0.2 | 0.881 | 9.0 | ± | 0.6 | 11.3 | ± | 4.2 | 1.4 | ± | 0.8 | 0.684 |
| LTR/ERVK-MYSERV6-int | 1.7 | ± | 0.3 | 5.7 | ± | 2.3 | 0.5 | ± | 0.3 | 0.887 | 4.7 | ± | 0.9 | 4.0 | ± | 1.5 | 1.3 | ± | 0.2 | 0.264 |
| DNA/TcMar-Tigger-Tigger1 | 0.3 | ± | 0.3 | 0.7 | ± | 0.7 | ND | ± | ND | ND | 1.3 | ± | 1.3 | 1.7 | ± | 0.7 | 1.3 | ± | 1.3 | 0.566 |
| LTR/ERVK-IAPLTR2_Mm | 0.0 | ± | 0.0 | 1.3 | ± | 0.3 | 0.0 | ± | 0.0 | 0.971 | 1.3 | ± | 0.9 | 2.0 | ± | 1.0 | 1.3 | ± | 0.9 | 0.629 |
| LTR/ERVK-IAPLTR2b | 0.3 | ± | 0.3 | 2.0 | ± | 0.6 | 0.2 | ± | 0.2 | 0.935 | 1.7 | ± | 0.9 | 1.3 | ± | 0.3 | 1.3 | ± | 0.9 | 0.371 |
| LTR/ERVK-MERVK26-int | 1.0 | ± | 0.0 | 1.0 | ± | 1.0 | ND | ± | ND | ND | 1.3 | ± | 1.3 | 2.7 | ± | 1.2 | 1.3 | ± | 1.3 | 0.687 |
| LTR/ERVK-RMER6D | 1.3 | ± | 1.3 | 2.7 | ± | 0.9 | 0.4 | ± | 0.4 | 0.772 | 3.0 | ± | 0.0 | 5.3 | ± | 2.2 | 1.3 | ± | 0.9 | 0.801 |
| LTR/ERVK-IAPEY4_I-int | 0.7 | ± | 0.3 | 1.7 | ± | 0.7 | 0.4 | ± | 0.3 | 0.887 | 2.0 | ± | 0.6 | 2.3 | ± | 0.9 | 1.3 | ± | 0.5 | 0.587 |
| LTR/ERVK-RLTR40 | 1.7 | ± | 0.3 | 1.3 | ± | 0.9 | ND | ± | ND | ND | 2.7 | ± | 1.2 | 2.0 | ± | 0.6 | 1.2 | ± | 0.2 | 0.211 |
| LTR/ERVK-RMER19B2 | 1.7 | ± | 0.9 | 4.3 | ± | 0.7 | 0.5 | ± | 0.3 | 0.896 | 2.7 | ± | 0.7 | 3.0 | ± | 1.5 | 1.2 | ± | 0.4 | 0.629 |
| Simple_repeat-(AG)n | 2.3 | ± | 0.9 | 5.3 | ± | 0.3 | 0.5 | ± | 0.2 | 0.939 | 1.7 | ± | 0.9 | 2.0 | ± | 0.6 | 1.2 | ± | 0.9 | 0.596 |
| LTR/ERVK-RMER17A2 | 0.7 | ± | 0.7 | 4.3 | ± | 0.9 | 0.1 | ± | 0.1 | 0.996 | 1.7 | ± | 0.9 | 1.7 | ± | 0.3 | 1.2 | ± | 0.6 | 0.500 |
| LTR/ERVL-RMER10B | 1.7 | ± | 0.9 | 2.3 | ± | 0.9 | 1.2 | ± | 0.6 | 0.636 | 1.3 | ± | 0.3 | 2.0 | ± | 1.5 | ND | ± | ND | ND |
| LINE/L1-L1MC3 | 0.3 | ± | 0.3 | 2.7 | ± | 0.9 | 0.3 | ± | 0.3 | 0.904 | 1.7 | ± | 0.7 | 3.3 | ± | 1.2 | 1.2 | ± | 0.9 | 0.768 |
| Simple_repeat-(TC)n | 2.0 | ± | 0.6 | 6.7 | ± | 2.2 | 0.4 | ± | 0.2 | 0.885 | 5.0 | ± | 1.5 | 6.0 | ± | 2.0 | 1.1 | ± | 0.5 | 0.661 |
| LTR/ERVK-RLTR45-int | 1.7 | ± | 0.3 | 8.0 | ± | 1.0 | 0.2 | ± | 0.0 | 0.991 | 4.0 | ± | 0.0 | 4.7 | ± | 1.5 | 1.1 | ± | 0.4 | 0.654 |
| LINE/CR1-L3 | 0.3 | ± | 0.3 | 1.0 | ± | 0.6 | ND | ± | ND | ND | 1.3 | ± | 0.3 | 1.7 | ± | 0.7 | 1.1 | ± | 0.5 | 0.629 |
| LTR/ERVL-MT2_Mm | 1.3 | ± | 0.9 | 6.0 | ± | 0.0 | 0.2 | ± | 0.1 | 0.983 | 5.0 | ± | 2.6 | 7.0 | ± | 2.1 | 1.1 | ± | 0.7 | 0.646 |
| LINE/L1-Lx2A | 0.0 | ± | 0.0 | 1.7 | ± | 0.9 | ND | ± | ND | ND | 1.3 | ± | 0.3 | 2.0 | ± | 1.0 | 1.1 | ± | 0.5 | 0.683 |
| LINE/L1-L1MB8 | 1.3 | ± | 0.9 | 2.0 | ± | 1.0 | 1.1 | ± | 1.0 | 0.654 | 1.7 | ± | 0.7 | 1.7 | ± | 0.9 | ND | ± | ND | ND |
| LTR/ERVL-MaLR-ORR1A0 | 1.3 | ± | 0.9 | 4.7 | ± | 2.2 | 0.6 | ± | 0.5 | 0.811 | 4.3 | ± | 0.3 | 4.7 | ± | 1.2 | 1.1 | ± | 0.3 | 0.580 |
| LTR/ERVK-ETnERV3-int | 1.7 | ± | 0.3 | 2.0 | ± | 0.6 | 1.1 | ± | 0.5 | 0.667 | 2.0 | ± | 0.6 | 1.7 | ± | 0.9 | ND | ± | ND | ND |
| LTR/ERVL-MT2C_Mm | 0.3 | ± | 0.3 | 4.7 | ± | 0.9 | 0.1 | ± | 0.1 | 0.965 | 2.7 | ± | 1.2 | 4.3 | ± | 1.5 | 1.0 | ± | 0.7 | 0.706 |
| LINE/L1-L1M2 | 3.3 | ± | 0.9 | 19.3 | ± | 1.8 | 0.2 | ± | 0.0 | 0.996 | 12.7 | ± | 4.2 | 15.0 | ± | 3.2 | 1.0 | ± | 0.5 | 0.614 |
| LINE/L1-L1MD | 1.0 | ± | 0.0 | 2.7 | ± | 1.5 | ND | ± | ND | ND | 2.7 | ± | 0.3 | 3.0 | ± | 1.0 | 1.0 | ± | 0.3 | 0.629 |

[a]10,000 randomly selected joined reads each from CENP-A native ChIP or input were submitted to RepeatMasker [S3].
[b]Repeats with an average fold-enrichment greater than 1 for either C57BL6/J or CHPO are reported in order of fold-enrichment (i.e., max of fold-enrichment for C57BL/6J and for CHPO). Repeat names correspond to those in the RepeatMasker library.
[c]Number of elements is reported as the mean ± sem, n = 3 independent replicates.
[d]Fold-enrichment was calculated for each replicate by dividing the number of elements in the CENP-A ChIP by the number in the input. The mean ± sem is reported.
[e]p-value reported is from a one-tailed t-test comparing the number of elements of CENP-A ChIP and input replicates. Performing a Bonferroni adjustment for multiple testing establishes a p-value of $\leq \alpha/n$ (0.05/43 = 0.0012) as significant. In CHPO, only minor and major satellite repeats meet this threshold. For C57BL/6J, the minor satellite fold-enrichment p-value of 0.003 does not meet the conservative threshold specified by Bonferroni adjustment. However, more than 6,000 minor satellite repeats were identified in 10,000 CENP-A ChIP reads, an order of magnitude more than any other repetitive element.
[f]Mouse minor satellite repeat
[g]Mouse major satellite repeat
ND, not determined. Either CENP-A ChIP or input value was 0 for one or more replicates.

**Table S2. Calculations for CENP-A nucleosome density at minor satellite array. Related to Figure 2.**

| | C57BL/6J | | CHPO | |
|---|---|---|---|---|
| Genome size, bp[a] | $2.7 \times 10^9$ | | $2.7 \times 10^9$ | |
| N, chromosomes[b] | 20 | | 13 | |
| Fraction minor satellite[c] | $5.3 \times 10^{-3}$ | | $4.0 \times 10^{-4}$ | |
| Average minor satellite array size per centromere, kb[d] | 716 | | 83 | |
| Nucleosome spacing, bp | from = 200 | to = 160 | from = 200 | to = 160 |
| **Nucleosomes at minor satellite array[e]** | **3578** | **4472** | **415** | **519** |
| CENP-A molecules at RPE centromere[f] | low = 180 | high = 580 | low = 180 | high = 580 |
| **CENP-A nucleosome count at stronger centromere[g]** | **90** | **290** | | |
| Factor = 1/(brighter/dimmer)[h] | | | factor = 0.75 | |
| **CENP-A nucleosome count at weaker centromere[i]** | | | **67** | **217** |
| | lowest est = | highest est = | lowest est = | highest est = |
| **Percent CENP-A nucleosomes at minor satellite[j]** | **2%** | **8%** | **13%** | **52%** |

[a]Estimate from [S4].

[b]Chromosome number. CHPO has 7 metacentric chromosomes.

[c]Estimated fraction of genome that is minor satellite based on MNase-seq results (Figure 2D).

[d]Average minor satellite array size in kb at centromeres was estimated as follows: mouse genome size (bp)/chromosome number x fraction of the genome that is minor satellite/1000

[e]The number of nucleosomes at the minor satellite array was estimated as follows: average minor satellite array size (bp) /nucleosome spacing (bp).

[f]The number of CENP-A molecules at human centromeres has been carefully measured [S5]. Here, we use minimum and maximum estimates for the number of centromeric CENP-A molecules reported in [S5] Figure 5G.

[g]We assume that C57BL/6J centromeres have a similar number of nucleosomes (molecules/2) of CENP-A as was observed at a typical human centromere.

[h]CHPO has less CENP-A nucleosomes per centromere than C57BL/6J by a factor of 1/median signal ratio = 1/1.336 (see Figure 4B).

[i]CENP-A nucleosome count at weaker centromeres was calculated as the CENP-A nucleosome count at stronger centromere x factor.

[j]CENP-A nucleosome count/nucleosomes at minor satellite array x 100%

**Supplemental References:**


S1. Hasson, D., Panchenko, T., Salimian, K.J., Salman, M.U., Sekulic, N., Alonso, A., Warburton, P.E., and Black, B.E. (2013). The octamer is the major form of CENP-A nucleosomes at human centromeres. Nat. Struct. Mol. Biol. *20*, 687–95.

S2. Masumoto, H., Yoda, K., Ikeno, M., Kitagawa, K., Muro, Y., and Okazaki, T. (1993). Properties of CENP-B and its target sequence in a satellite DNA. In NATO ASI Series Volume 72 (Berlin, Heidelberg: Springer Berlin Heidelberg), pp. 31–43.

S3. Smit, A., Hubley, R., and Green, P. RepeatMasker Open-4.0. 2013-2015 <http://www.repeatmasker.org>.

S4. Chinwalla, A.T., Cook, L.L., Delehaunty, K.D., Fewell, G.A., Fulton, L.A., Fulton, R.S., Graves, T.A., Hillier, L.W., Mardis, E.R., McPherson, J.D., *et al.* (2002). Initial sequencing and comparative analysis of the mouse genome. Nature *420*, 520–562.

S5. Bodor, D.L., Mata, J.F., Sergeev, M., David, A.F., Salimian, K.J., Panchenko, T., Cleveland, D.W., Black, B.E., Shah, J. V, and Jansen, L.E. (2014). The quantitative architecture of centromeric chromatin. Elife *3*, e02137.